Pharmaceutical Research, Vol. 22, No. 1, January 2005 (© 2005)
DOI: 10.1007/s11095-004-9010-6

Research Paper

Selective Downregulation of Hepatic Cytochrome P450 Expression and Activity in a Rat Model of Inflammatory Pain

Denis Projean,[1,2] Sophie Dautrey,[2] Huy Khan Vu,[2] Thierry Groblewski,[2] Jean-Louis Brazier,[1] and Julie Ducharme[1,2,3]

Received May 29, 2004; accepted September 12, 2004

Purpose. This study was designed to examine the effect of Freund's complete adjuvant (FCA)-induced inflammation on liver P450 expression and activities in the first 7 days that followed a single FCA injection in the rat hindpaw.
Methods. Rats were humanely sacrificed at regular time points, plasma and liver samples were collected, liver mRNA extracted, and liver microsomes prepared.
Results. FCA injection led to the development of an acute inflammatory response evidenced by paw edema and increased alpha-1-acid glycoprotein (AGP) and total-nitrite (NOx) plasma concentrations. Plasma IL-6 levels were significantly higher in FCA-treated rats than in controls at 8 h post-FCA. Within 24 h, these changes were accompanied by a rapid decrease in total P450 contents in FCA-treated rat liver and the selective downregulation of specific CYP isoforms, as illustrated by decreased mRNA levels (CYP2B, CYP2C11, CYP3A1, and CYP2E1), protein contents (CYP2B, CYP2C11, and CYP2E1) or catalytic activities (CYP2C6, CYP2C11, and CYP2E1). CYP3A1 mRNA levels were severely decreased by FCA administration, whereas CYP3A2 mRNA and protein levels remained unchanged.
Conclusions. These early biochemical and metabolic modifications may have pharmacokinetic and pharmacodynamic consequences when hepatically cleared drugs are administered to FCA-treated rats, especially within the first 24–72 h post-FCA.

KEY WORDS: cytochrome P450; Freund's complete adjuvant; inflammation; interleukin-6; rat.

INTRODUCTION

Cytochromes P450 (P450s) constitute a superfamily of enzymes that catalyze a variety of oxidative reactions, including xenobiotic biotransformation and endogenous substrate synthesis or catabolism. In mammals, the CYP families primarily involved in drug metabolism include the CYP1, CYP2, CYP3, and to a lesser extent the CYP4 family. Their expression and activity are influenced by a variety of events such as genetic, endogenous, environmental, or pathophysiological factors (1). For instance, infectious and inflammatory stimuli, by triggering a series of events collectively called the acute phase response, can lead to altered drug metabolism and pharmacokinetics and eventually influence clinical response (2).

In drug development, designing an effective strategy for testing new analgesics is highly dependent upon our ability to develop preclinical pain models that will reproduce persistent pain conditions in man. For instance, in rodents, a variety of stimuli can be used to elicit inflammatory conditions but the extent of tissue damage, inflammation severity and duration as well the appearance of hyperalgesia and/or allodynia will vary significantly depending on the model (3). Lipopolysaccharides (LPS), turpentine, or particulate irritants can trigger a marked inflammatory reaction but are rarely used as pain models because of their extreme severity. At lower doses that are not associated with severe tissue injury, carrageenan-induced paw edema is a model of inflammation rather than a pain model. In contrast, a single FCA injection in the rat hindpaw has been shown to produce a stable and reproducible thermal hyperalgesia from 24 to 72 h postadministration with no other macroscopic changes than paw redness and edema (4,5).

When FCA is administered into the joint or at the tail base, acute inflammation progresses slowly to a complex ar-

[1] Faculté de Pharmacie, Université de Montréal, Montréal, Québec, Canada.
[2] AstraZeneca R & D Montréal, Ville St-Laurent, Québec, Canada.
[3] To whom correspondence should be addessed. (e-mail: julie.ducharme@astrazeneca.com)

ABBREVIATIONS: AGP, α_1-acid glycoprotein; ANOVA, analysis of variance; API-ES, atmospheric pressure ionization–electrospray; CYP, cytochrome P450 isoform; DM, dextromethorphan; DEX, dextrorphan; DF, diclofenac; ELISA, enzyme-linked immunosorbent assay; FCA, Freund's complete adjuvant; HPLC/MS, high-performance liquid chromatography/mass spectrometry; 4-OH-DF, 4-hydroxydiclofenac; IL, interleukin; LOQ, limit of quantification; LPS, lipopolysaccharide (*E. coli* endotoxin); M, mass of the parent compound; MH+, molecular ion; m/z, mass over charge ratio; MS, mass spectrometry; NADPH; nicotinamide adenosine diphosphate reduced form; NOx, total nitrite levels; P450; cytochrome P450; SIM, selected ion monitoring; SDS, sodium dodecyl sulfate; TNF-α, tumor necrosis factor-α.

thritis-like stage in 14 days or more postinjection (6). This FCA-induced arthritis has been recognized to decrease total P450 contents in rat liver (7). Despite a broad characterization using nonspecific P450 substrates such as aminopyrine (7), a systematic evaluation of FCA-mediated downregulation of hepatic individual P450 activities/contents has never been reported in the rat. Moreover, such studies have not been performed in the FCA-induced hyperalgesia model when rats are tested in the early days following FCA injection and do not show arthritis-like symptoms.

Because of the importance of the FCA-induced hyperalgesia model in pain research and its widespread use in the pharmacodynamic characterization of a broad range of analgesics, we characterized the biochemical and metabolic events that occur during the acute inflammation phase triggered by a single FCA injection to rats, and assessed their potential impact on drug metabolism and pharmacokinetics. To address this, we examined the effect of FCA-induced inflammation on rat hepatic P450 mRNA levels, protein contents, and activities in the first 7 days that followed FCA administration. In addition, using a combination of biochemical assays and highly specific HPLC-UV or HPLC-MS methods, we evaluated the relationships between the observed modifications in P450 contents/activities with the time-course of selected inflammatory mediators.

MATERIALS AND METHODS

Chemicals

Diclofenac (DF), dextromethorphan (DM) hydrobromide, dextrorphan (DEX), *p*-nitrophenol, *p*-nitrocatechol, Tween 20, and *Mycobactrium tuberculosis* were purchased from Sigma-Aldrich (Oakville, Ontario, Canada). Androstenedione, testosterone and its hydroxylated metabolites (2α, 2β, 6β, 7α, 16α, and 16β hydroxytestosterone) were obtained from Steraloids (Wilton, NH, USA). Four-hydroxydiclofenac (4-OH-DF) was obtained from BDGentest (Woburn, MA, USA). All other chemicals were obtained from VWR International (Montréal, Québec, Canada).

Animals and Treatments

The experimental protocol was approved by the Institutional Animal Care and Use Committee of AstraZeneca R&D Montréal. All procedures were conducted according to CCAC (Canadian Council on Animal Care) and AAALAC (Association for the Assessment and Accreditation of Laboratory Animal Care) guidelines. Male Sprague-Dawley rats (Charles River, St-Constant, Québec), weighing 170–220g, were housed under standard conditions (light/dark cycle of 12 h; room temperature of ~20°C) and provided with food and water *ad libitum*. FCA was prepared from 1-mg heat killed *Mycobaterium Tuberculosis* dissolved in a mixture of 0.85 ml of paraffin oil and 0.15 ml of mannide oleate. FCA-treated rats received a single subcutaneous injection of 100 μl of FCA into the plantar face of the left hindpaw. Control rats were treated with an equal volume of saline. In a first set of rats, hindpaw volumes were measured by liquid plethysmometry (Ugo Basile, Comerio, Italy) 24, 48, 72, and 168 h after the injection of FCA or saline (n = 6/group). Following isoflurane anesthesia, the same animals were killed by cardiac puncture (exsanguination) and blood was collected in EDTA tubes. In addition, livers were removed immediately following cardiac puncture, washed to remove excess blood, frozen in liquid nitrogen and stored at −80°C until microsome preparation. In a second set of rats (n = 6/group), only blood samples were collected by cardiac puncture under light anesthesia, in EDTA tubes 4, 8, and 12 h after the injection of FCA. Plasma obtained following blood centrifugation (3000 × *g* for 15 min) was stored at −80°C.

Determination of Total Nitrite Levels (NOx)

Nitrite, a stable end product of nitric oxide, was measured in rat plasma using a commercially available kit (Oxis International inc, Portland, OR, USA). Plasma (5 μl) was incubated with nitrate reductase to reduce any nitrates to nitrites. Following incubation, samples were treated with Griess reagent and absorbance was measured at 540 nm. The limit of quantification (LOQ) was 10 μM.

Determination of α_1-acid Glycoprotein (AGP) Levels

AGP was measured in rat plasma using a commercially available radial immunodiffusion kit (Cardiotech service, Louisville, KY, USA). The LOQ was 100 μg/ml.

Determination of Cytokine Levels

Interkeukin (IL)-1β, IL-6 and tumor necrosis factor (TNF)-α levels were determined using rat-specific ELISA kits (Endogen, Woburn, MA, USA; Amersham Bioscience, Baie d'Urfé, Québec, Canada). The LOQ was 25 pg/ml for IL-1β and 31 pg/ml for both IL-6 and TNF-α. Cytokines were assayed at all time points.

RNA Isolation

Total RNA from approximately 1 g of rat liver was extracted using Maxipreps RNEasy kits (Qiagen, Mississauga, Canada) according to the manufacturer's instructions. A total of 20 livers from five treatment groups were processed (n = 4 per group): saline injection controls, 24, 48, 72, and 168 h following FCA injection. Contaminating genomic DNA was removed by On-Column DNase digestion (Qiagen) with the RNase-Free DNase Set (82 Kunitz units of DNase per column, incubated for 15 min at room temperature according to the supplier's recommendations).

Reverse-Transcriptase cDNA Synthesis

Total RNA from each sample was reverse-transcribed into first-strand cDNA with the 1st Strand cDNA Synthesis Kit for RT-PCR (Roche, Laval, Canada) according to the manufacturer's instructions (1 μg of DNase I-treated total RNA in a total volume of 20 μl). Poly dT oligonucleotide was used to prime the synthesis. Before RT-PCR amplification, all the cDNA sample volumes were adjusted to 40 μl with water.

Real-time PCR Amplification and Quantification

Five pairs of specific primers for rat CYP isoforms (CYP2B1/B2, CYP2E1, CYP2C11, CYP3A1, CYP3A2) and one pair of primers for the housekeeping gene (cyclophilin) were obtained from a Rat Cytochrome P450 Competitive RT-

PCR Set (Takara Bio Inc., Shiga, Japan, cat. no. 6608). PCR amplification was performed using the LightCycler instrument (Roche). For each pair of primers optimal MgCl2 concentration and annealing temperature were experimentally determined: the optimal MgCl2 concentration was 5 mM for CYP2B1/B2, CYP3A2 and cyclophilin, 3 mM for CYP2C11, and 2 mM for both CYP2E1 and CYP3A1 primers. The annealing temperature was set at 56°C for all primers except CYP2B1/B2 (59°C). The reaction mixture consisted of 1 μl cDNA, 0.5 μM each primer, and 2 μl LightCycler FastStart DNA Master SYBR Green 1 mix containing dNTPs, SYBR Green I dye in a 10 mM $MgCl_2$ solution (Roche). Final volume was adjusted to 20 μl with water.

All cDNAs were amplified using the following LightCycler protocol: the FastStart polymerase was activated for 10 min at 96°C and the DNA template was amplified for 45 cycles [including DNA denaturation (10 s at 96°C), annealing of the primers (5 s at 56°C or 59°C, see above for details) and DNA polymerization (25 s at 72°C)]. Fluorescence data were acquired at the end of each extension phase. At the end of the last cycle, temperature was raised gradually (0.2°C/s) from the annealing temperature to 96°C to determine the melting point of PCR products. Product identity was confirmed by gel electrophoresis and melting curve analysis. All amplification signals were normalized against the cyclophilin mRNA contents of the sample. Generation of calibration curves and semi-quantification of specific rat CYP isoform mRNA was performed with the LightCycler software (version 3.5, Roche). Within the same treatment group, outliers (deviating from mean values by more than 2 standard deviations) were rejected from data analysis.

Preparation of Rat Liver Microsomes

Rat liver microsomes were prepared by differential ultracentrifugation according to the method of Pearce *et al.* (8). The final microsomal pellets were resuspended in 0.25 M sucrose and stored at −80°C. Microsomal proteins were measured by the BCA protein assay (Pierce, Woburn, MA, USA) using bovine serum albumin solutions as standards. Cytochrome P450 quantification was carried out according to the method of Omura and Sato (9).

Gel Electrophoresis and Western Immunoblotting

Protein levels of various CYP isoforms present in rat liver microsomes were measured by western immunoblotting. Proteins (samples and standards) were separated by SDS polyacrylamide gel electrophoresis (10% polyacrylamide) and transferred onto a nitrocellulose membrane (Invitrogen, Burlington, Ontario, Canada). Phenobarbital-induced (CYP2B and CYP3A2) and benzphetamine-induced (CYP2C11) rat liver microsomes were used as standards and were provided by the antibodies supplier (BDGentest, Woburn, MA, USA). For CYP2E1, recombinant rat CYP2E1 was used as standard (BDGentest, Woburn, MA, USA). Immunoblots were performed in 5% non-fat milk in PBS and washed in PBS containing 0.1% Tween 20. Membranes were then incubated with polyclonal goat anti-rat CYP2B1, CYP2C11, CYP2E1, or CYP3A2 primary antibodies (1:1000; BDGentest Woburn, MA, USA). Anti-rat CYP2B1 has been shown to cross-react with CYP2B2 and the 10% polyacrylamide gel could not clearly separate the bands. Thus, the bands recognized by the anti-CYP2B1 antibody were regarded as CYP2Bs. Immune complexes were revealed using rabbit anti-goat IgG (secondary antibody; 1:10,000) coupled to horseradish peroxydase (Sigma-Aldrich, Oakville, Ontario, Canada). The binding of all antibodies was detected using electrochemiluminescence (LumiGLO, Kirkegaard & Perry Lab, Gaithersburg, MD, USA) onto an Hyperfilm ECL autoradiography film (Amersham bioscience, Baie d'Urfé, Québec, Canada). The product intensities of the immunoblots were measured with a Hewlett Packard Scanner (Hewlett Packard, Kirkland, Québec, Canada) equipped with the PC version of Scion Image/Gel analysis program (Scion Corp, Frederick, MD, USA). Band intensities were normalized to that of a standard that was run in the same gel.

Testosterone Hydroxylase Assay

An incubation mixture containing KH_2PO_4 (0.1 M pH 7.4), testosterone (250 μM) and liver microsomes (0.3 mg/ml final protein concentration) was pre-incubated for 5 min at 37°C. The enzymatic reaction was initiated by the addition of NADPH (1 mM final) and was allowed to proceed for 10 min. The final assay volume was 500 μl and final solvent concentration (methanol) was less than 1%. Control incubations were performed to ensure product formation linearity against time and protein concentration. The reaction was stopped with the addition of an equal volume of ice-cold methanol. Samples were then vortex-mixed, put on ice for 10 min and centrifuged (3500 × *g* for 30 min at 4°C). Supernatants were frozen until HPLC analysis.

Testosterone and its hydroxylated metabolites were quantified using an HPLC-UV method adapted from Whalley *et al.* (10). Briefly, an aliquot (50 μl) of the supernatant was injected onto a reversed-phase HPLC column (Hypersil BDS C-18 analytical column 3 μm, 4.6 × 100 mm; Phenomenex, Torrance, CA, USA) and eluted with a linear step gradient of tetrahydrofuran-acetonitrile-water (10:10:80 changing to 14:14:72 over 10 min) followed by an isocratic hold of 5 min. The total run time was 15 min. The mobile phase was allowed to re-equilibrate for 3 min between injections. The flow rate was 1.25 ml/min. Retention times were 3.1 min for 7α-testosterone, 3.7 min for 6β-testosterone, 4.2 min for 16α-testosterone, 5.5 min for 16β-testosterone, 6.2 min 11β-testosterone, 6.5 min for 2α-testosterone, 6.8 min for 2β-testosterone, 10.6 min for androstenedione, and 11.3 min for testosterone. Analytes were detected at 255 nm. The method was linear between 78 and 40,000 nM for all metabolites (R^2 = 0.999), mean accuracy averaged 95%, and intra-day reproducibility was within 10%. The LOQ of the method was 78 nM for all metabolites.

Diclofenac 4-Hydroxylase and Dextrometorphan *O*-demethylase Assays

An incubation mixture containing KH_2PO_4 (0.1 M pH 7.4), DF (25 μM) or DM (10 μM), and liver microsomes (0.3 mg/ml final protein concentration) was pre-incubated for 5 min at 37°C. The enzymatic reaction was initiated by the addition of NADPH (1 mM final) and was allowed to proceed for 15 (DM) or 30 min (DF). The final incubation volume was 500 μl and final solvent concentration (DMSO) was less than

1%. Control incubations were performed to ensure product formation linearity against time and protein concentration. Reactions were stopped by the addition of an equal volume of ice-cold acetonitrile. Samples were then vortex-mixed, put on ice for 10 min and centrifuged (3500 × *g* for 30 min at 4°C). Supernatants were frozen until HPLC analysis.

DEX and 4-OH-DF were quantified using an HPLC/MS method developed in our laboratory. Supernatants (5–20 μl) were injected directly into the HPLC/MS system [Agilent 1100/Benchtop MS detector equipped with an electrospray source (Agilent Technology, Ville St-Laurent, Québec, Canada)]. Chromatographic separations were achieved on a reversed-phase HPLC column (Inertsil-ODS-3 C18, 3 μm, 4.6 × 75 mm; Agilent Technology). The mobile phase consisted of a mixture of 0.1% formic acid in acetonitrile (A) and 0.1% formic acid in water (B). From 0 to 0.5 min, the mobile phase was kept at 100% B and from 0.5 to 5 min, a linear gradient of A into B (5 to 95%) was run. The total run time was 7 min. The mobile phase was allowed to re-equilibrate for 3 min between injections. The flow rate was 1 ml/min. Retention times were 2.88 min for DEX, 5.0 min for 4-OH-DF, 3.25 min for DM, and 6.0 min for DF. The MS detector was set in selected ion monitoring (SIM) mode for the quantitative analysis of DEX and 4-OH-DF (m/z = MH^+, M being the mass of the parent compound; m/z = 296 for DF, m/z = 312 for 4-OH-DF, m/z = 272 for DM, and m/z = 258 for DEX). Nebulizer pressure was 60 psi while the drying gas (nitrogen) was delivered at 13 L/min. Capillary voltage was 3500 V and the fragmentor collision-induced dissociation cell was set at 70 V. Analytes were identified on the basis of their retention times and mass spectra compared to standard solutions. Calibration curves (4.88–10,000 nM) were constructed by quadratic regression of the analyte peak area vs concentration curves (using a weighting factor of 1/concentration). Regression coefficients were always higher than 0.999. Mean intraday variation was less than 10%, accuracy averaged 95% and the LOQ was 4.88 nM.

p-Nitrophenol Hydroxylase Assay

An incubation mixture containing KH_2PO_4 (0.1 M pH 7.4), *p*-nitrophenol (100 μM), and liver microsomes (0.3 mg/ml final protein concentration) was pre-incubated for 5 min at 37°C. The enzymatic reaction was initiated by the addition of NADPH (1 mM final) and was allowed to proceed for 30 min. The final assay volume was 500 μl. Control incubations were performed to ensure product formation linearity against time and protein concentration. The reaction was stopped with the addition of 100 μl of trichloroacetic acid (20% v/v). Samples were then vortex-mixed, put on ice for 10 min and centrifuged (3500 × *g* for 30 min at 4°C). Supernatant aliquots (125 μl) were transferred into a polystyrene 96-well plate and diluted with 62.5 μl of NaOH (2 mM). The plate was shaken briefly and absorbance was measured by spectrophotometry at 535 nm.

Data Analysis

Cytochrome P450 protein levels, mRNA contents, total P450 contents and P450 activities were expressed as percentages of the mean of the control group. Differences between FCA-treated and control groups were analyzed by one-way analysis of variance (ANOVA) followed by the Dunnett *post hoc* test. The level of significance was set at 0.05.

RESULTS

Inflammatory Mediators in FCA-Treated Rats

In the early days following injection, FCA administration is associated with local inflammatory signs such as edema, erythema and hyperalgesia (5). In our study, FCA injection led to the development of an acute inflammatory response, as evidenced by paw edema and increased AGP and NOx levels. Indeed, all FCA-treated rats showed significant paw edema (measured by paw volume in comparison to control rats) (Fig. 1A). From 24 h to 7 days after FCA treatment, NOx plasma levels were found to be significantly higher in FCA-treated than in control rats (Fig. 1B). Peak NOx levels (287 ± 24 μM) occurred at 72 h post-FCA administration. AGP levels were also significantly increased in FCA-treated rats between 24 and 72 h post-FCA. AGP levels decreased to control levels 7 days after the FCA injection (Fig. 1B). IL-6 could not be detected in any plasma samples from control rats (<31 pg/ml). In FCA-treated animals, IL-6 levels were detectable at 8 h postinjection (219 ± 70 pg/ml). TNF-α and IL-1β concentrations were found to be below the limit of detection in all plasma samples (FCA-treated and control rats).

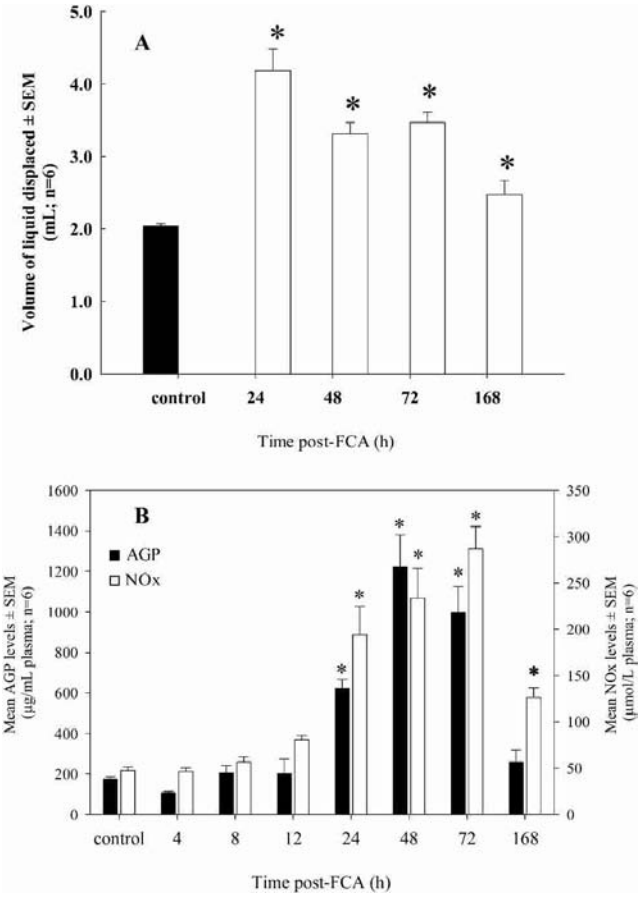

Fig. 1. (A) Volume of liquid displaced by the left hindpaw following a subcutaneous administration of saline (control; □) or FCA (■) to rats. (B) Nitrite + nitrate (NOx) and AGP levels in plasma following a subcutaneous administration of saline (control; □) or FCA (■) to rats. *$p < 0.05$: control vs. FCA-treated rats.

mRNA Levels of Specific CYP Isoforms in Rat Livers

The mRNA levels of CYP2C11, CYP3A1, CYP3A2, CYP2Bs, and CYP2E1 in livers obtained from rats sacrificed at different time points following FCA or saline administration were determined by RT-PCR (Fig. 2). Except for CYP3A2 mRNA, which appeared unaltered by FCA treatment, all other CYP isoforms were associated with significantly decreased mRNA levels at 24 h post-FCA. For CYP3A1 and CYP2B mRNA, this decrease was still significant at 48 and 72 h post-FCA, respectively. At 7 days post-FCA, all CYP mRNA levels were back to control values except for CYP2B1, which remained at 54% of controls. Indeed, CYP3A1 mRNA appeared to be the most affected by FCA

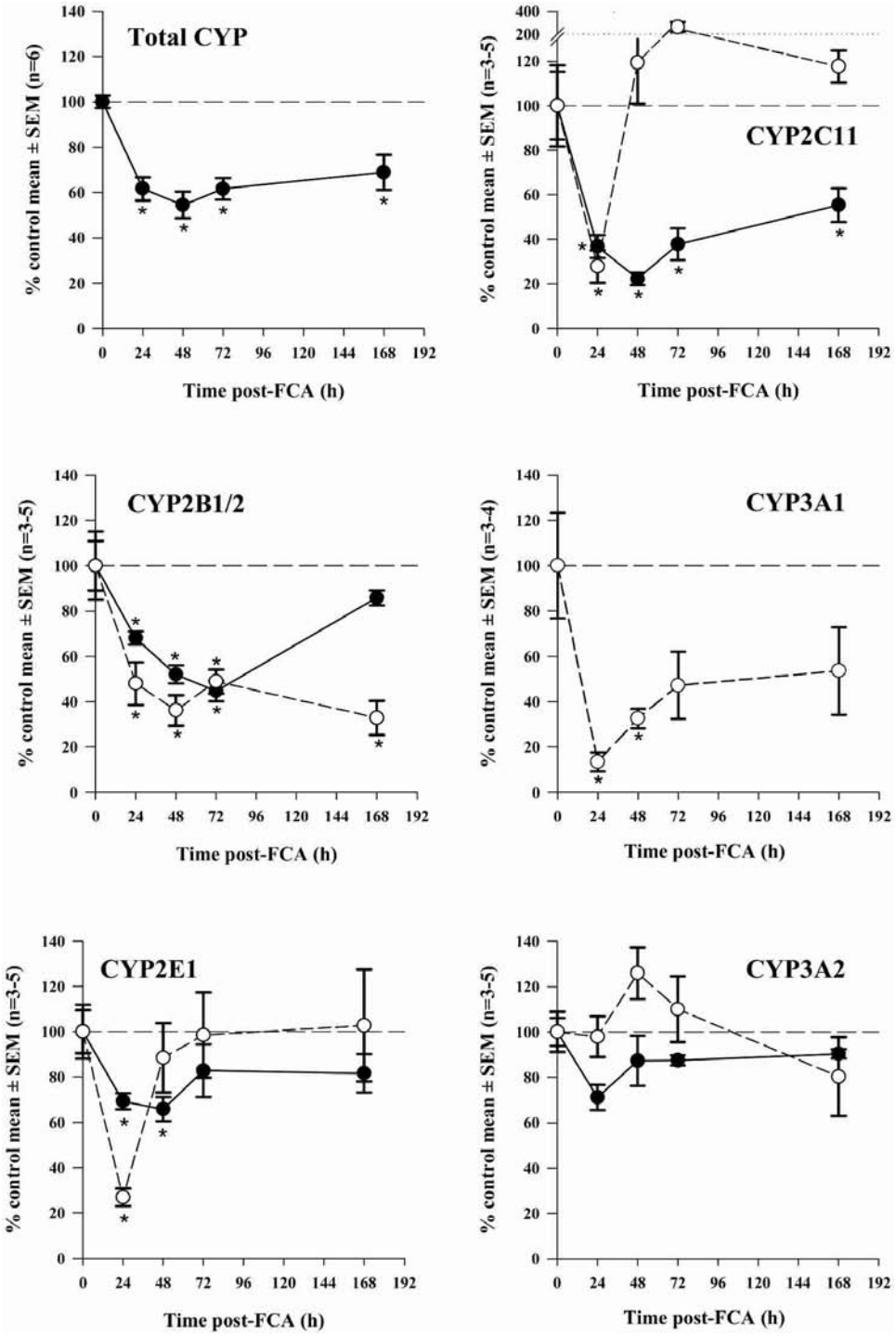

Fig. 2. CYP2Bs, CYP2C11, CYP2E1, CYP3A1, and CYP3A2 mRNA contents (○) in rat liver following a subcutaneous administration of saline/FCA to rats. mRNA levels were measured by RT-PCR and normalized for cyclophilin contents. Total CYP and CYP2Bs, CYP2C11, CYP2E1, and CYP3A2 microsomal protein levels (●) in rat liver following a subcutaneous administration of saline/FCA to rats. *$p < 0.05$: control vs. FCA-treated rats.

administration, down to 13% of control levels at 24 h post-FCA, followed by CYP2C11 and CYP2E1 (down 27% of controls), and by CYP2Bs (down to 46% of controls). Despite a steep decline at 24h post-FCA, CYP2C11 AND CYP2E1 mRNA were back to control values by 48 h and CYP2C11 levels even transiently increased up to 240% of control values at 72 h post-FCA.

Total CYP Levels and Individual Protein Contents in Rat Liver Microsomes

In rats treated with FCA, total P450 contents were significantly decreased when compared to controls (Fig. 2). In agreement with literature values, mean P450 contents were ~0.6 nmol/mg protein for the control group (11). Weak but significant correlations were observed between total P450 contents in liver microsomes and NOx or AGP plasma levels ($r = -0.52$ and -0.60, respectively; $p < 0.01$). Western blots of CYP2C11, CYP3A2, CYP2Bs, and CYP2E1 in liver microsomes obtained from rats sacrificed 72 h following FCA or saline administration are shown in Fig. 3. As with mRNA, all CYP protein levels except CYP3A2 were significantly decreased by FCA treatment, at 24 and 48 h postinjection. CYP2B levels were decreased to 40% of control values at 72 h post-FCA and were back to control levels after 7 days. CYP2E1 protein contents were decreased to ~60% of control levels at 48 h post-FCA and were also back to baseline after 7 days. CYP2C11 protein levels were the most severely affected by FCA administration, down to 23% of control values at 48 h. CYP2C11 protein levels were not back to baseline levels 7 days post-FCA (~60% of controls).

Testosterone Hydroxylation in Rat Liver Microsomes

In rats, CYP2B, CYP2C11 and CYP3As have been to shown to catalyze the hydroxylation of testosterone at the 16β, 2α/16α and 6β positions, respectively (12). Up to 72 h post-FCA, CYP2C11-related activities were lower in microsomes from FCA-treated rats than in controls (Fig. 4). At 48 h post-FCA, testosterone 2α and 16α-hydroxylase were severely affected, with a 70% decrease in activity compared to controls. At 7 days post-FCA, CYP2C11-related activities were back to control values. FCA did not have any significant influence on testosterone 6β-hydroxylase (CYP3As) (Fig. 4). Because constitutive CYP2B expression is very low in livers from uninduced rats, 16β-hydroxytestosterone levels were below the LOQ in all samples and no activity could be measured.

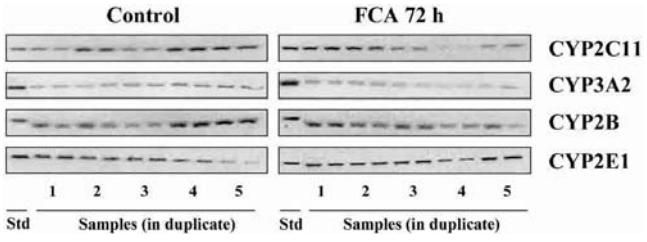

Fig. 3. Western blotting analysis of hepatic microsomal CYP isoforms obtained from control and FCA-treated (72 h) rats. Microsomes were subjected to SDS-PAGE electrophoresis and probed for different protein CYPs using anti-rat polyclonal antibodies. 625 to 2500 ng (CYP2B1/2, 2C11, 2E1, and 3A2) of microsomal proteins were loaded in each lane.

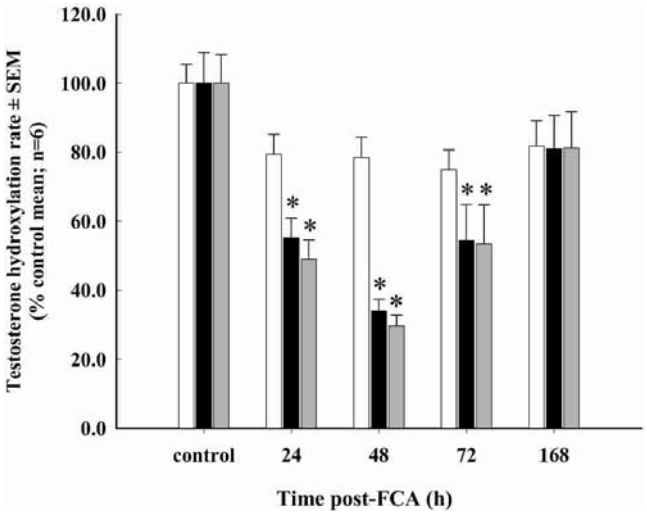

Fig. 4. Rates of 6β (□), 16α (■), and 2α (■) hydroxytestosterone formation in rat liver microsomes following a subcutaneous administration of saline (control) or FCA to rats. *$p < 0.05$: control vs. FCA-treated rats.

Other CYP Activities in Rat Liver Microsomes

DF 4-hydroxylation was significantly altered in rats treated with FCA when compared to controls (Fig. 5). This CYP2C6-related activity decreased to a maximum of 65% of control values at 24 h post-FCA. After 7 days, DF hydroxylase activity was back to control values. In addition, FCA administration significantly decreased the hydroxylation of *p*-nitrophenol (CYP2E1) at 24 and 72 h post-FCA (Fig. 5). In contrast, DM *O*-demethylation was not altered in liver microsomes obtained from FCA-treated rats compared to controls (Fig. 5).

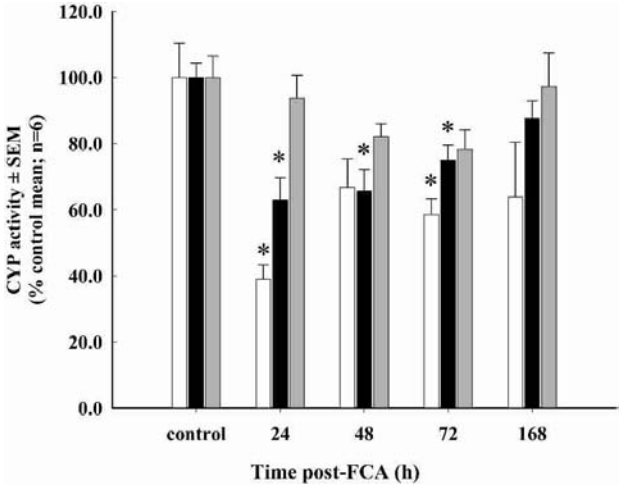

Fig. 5. *p*-Nitrophenol hydroxylase (□), dextromethorphan-*O*-demethylase (■), and diclofenac-4-hydroxylase (■) activities in rat liver microsomes following a subcutaneous administration of saline (control) or FCA to rats. *$p < 0.05$: control vs FCA-treated rats.

DISCUSSION

In this study, we showed that in rats, a single dose of FCA initiates an inflammatory reaction characterised by macroscopic changes at the site of injection (paw oedema) and increases in plasma concentrations of IL-6, NOx, and AGP. In turn, this inflammatory process triggers the downregulation of hepatic P450 expression in the first days following FCA administration. The observed decrease in total P450 protein levels (30–45% at 2–3 days post-FCA) appears to be more modest than that reported in FCA-arthritic rats (85% at 14 days post-FCA) (7), but comparable to that detected 24 and 48 h after the administration of turpentine, another rat model of acute local inflammation (13). Similarly, the release of pro-inflammatory cytokines appeared to be more important in FCA-arthritic rats (14), where TNF-α and IL-6 were increased 14 to 25 days after FCA injection, than in our FCA-treated rats, where only increases in IL-6 could be detected at 8 h postinjection. Our results also demonstrate that FCA-induced inflammation has a selective influence on CYP expression and/or activity in rat liver, as illustrated by decreased mRNA levels (CYP2B, CYP2C11, CYP3A1, and CYP2E1), protein contents (CYP2B, CYP2C11, and CYP2E1) or catalytic activities (CYP2C6, CYP2C11, and CYP2E1).

Literature findings in other rat models of acute inflammation confirm the major impact of inflammation on CYP2C11, CYP2E1, and to a lesser extent on CYP2B. In turpentine-treated rats, liver CYP2C11 contents were severely decreased 24 to 48 h after injection (13). In rats submitted to peritoneal macrophage stimulation by particulate irritants, CYP2C11 (mRNA and protein) liver expression was profoundly suppressed after 24 h (15). In livers from LPS-treated rats sacrificed at 24 h postinjection, CYP2C11, CYP2B, and CYP2E1 were diminished (16–18). In this study, some observations evidence some commonalities between CYP2B, CYP2E1 and CYP2C11. First, diminutions in protein levels were always paralleled or even preceded by a fast decrease in mRNA contents, suggesting that the effect triggered by FCA administration takes place mainly at the pre-translational level. Second, following the rapid initial decrease, protein levels usually started to increase within 48–72 h after FCA administration, evidencing the transient effect of the acute inflammatory response on the contents of some individual P450s.

For CYP2C11, the steep decline in mRNA observed at 24 h post-FCA was not only followed by a rapid return to baseline levels within 48 h but also by a sharp, transient increase in mRNA levels (up to 240% of control values) at 72 h. The mechanism(s) underlying this sudden activation of the transcriptional machinery following an initial suppression is(are) still poorly understood. Although any explanation is still speculative, this phenomenon could result from a redistribution of the same effectors involved in the initial CYP downregulation in response to the rapid decrease in protein contents or the clearance of the ligand(s) responsible(s) for triggering the initial down-regulation. Interestingly, in spite of this mRNA upregulation, CYP2C11 protein levels did not return to baseline (remaining at 60% of control levels after 7 days), suggesting that post-translational events are likely to play an important role in controlling CYP2C11 levels by modulating protein stability and/or maturation. Because CYP2C11 protein contents were so severely diminished in FCA-treated rat liver, even at 7 days post-FCA, and because this isoform is the major P450 constitutively expressed in male rat liver (13,19), the significant decrease in total P450 contents in livers from FCA-treated rats is likely to result from decreased CYP2C11 protein levels.

For CYP3A isoforms, literature reports show mixed findings depending on the inflammatory stimulus. Similar to our results obtained in FCA-treated rats, CYP3A2 mRNA and protein levels remained unchanged in rats submitted to peritoneal macrophage stimulation by particulate irritants (15). In contrast, in livers from rats treated with high doses of LPS and sacrificed at 24 h post-injection, CYP3A2 mRNA and/or protein levels were diminished, probably because of the severity of the systemic inflammatory reaction (15,16,20). Under our experimental setting, we were able to show distinct patterns of expression for two CYP3A isoforms. CYP3A1 mRNA was profoundly suppressed in FCA-treated rats while CYP3A2 mRNA was not significantly affected. To our knowledge, this is the first time that important differences between CYP3A1 and CYP3A2 gene regulation are evidenced in a model of inflammation, in the context of a downregulation. A differential expression of *CYP3A* genes is, however, well documented in the field of induction (21). In fact, CYP3A2 has been shown to be more refractory to induction following treatment with classic CYP inducers compared to CYP3A1 or CYP3A23 (CYP3A1 shows a six-base deletion vs. CYP3A23 and both genes appear to be regulated similarly) (22). Functional studies suggested that the reduced responsiveness of CYP3A2 to dexamethasone compared to CYP3A23 could be mediated by selective and preferential binding of nuclear receptor (PXR/RXR, COUP-TF, and HNF4) and/or ligand activating proteins to functional elements such as Dex-RE1, Dex-RE2 and site A (21). Because a plethora of nuclear receptors or transcription factors involved in CYP2B, CYP3A, CYP2C, or CYP2E1 gene functions (23) appear to be downregulated or upregulated following an acute inflammatory reaction (24–26), it is possible that the affinity of these effectors (nuclear receptors and/or transcription factors) for CYP3A2 regulating elements are responsible for its apparent resistance to both downregulation and induction.

This paper demonstrates that FCA-induced inflammation not only affects P450 expression at the message and protein levels but also P450-mediated oxidative activities. In male rat liver, testosterone 6-β hydroxylation is thought to be driven mainly by CYP3A2 activity since the latter represents the major CYP3A isoform and CYP3A1 protein expression is low (27). Therefore, consistent with the stability of CYP3A2 mRNA and protein levels, CYP3A-specific activity as measured by testosterone 6-β hydroxylation remained unchanged by FCA treatment, throughout the time-course of the experiment. In contrast, testosterone 2α/16α-hydroxylation rates, which are CYP2C11-specific activities, were severely diminished in FCA-treated rats, in agreement with the important downregulation in CYP2C11 protein contents.

CYP2E1 was the only isoform for which the magnitude of FCA-induced decreases in protein contents did not completely agree with the reduction in catalytic activity, as measured by *p*-nitrophenol hydroxylase activity. Overall, CYP2E1 activity tended to decrease more than protein contents. Although this could be explained, in part, by inter-individual variability, this could also be due to the regulation of CYP2E1, which may involve several mechanisms both at

the transcriptional and post-translational levels (24). For instance, Oesh-Bartlomowicz and Oesch have shown that some P450s, in particular CYP2B and CYP2E1, can be inactivated post-translationally without any decrease in their protein contents, through phosphorylation on a serine residue by cyclic AMP dependent protein kinases (28). Therefore, it is possible that the inflammatory processes triggered by FCA activate mechanisms that decrease CYP2E1 catalytic activity or protein turnover.

Several lines of evidence suggest that pro-inflammatory cytokines such as IL-6, IL-1β, and TNF-α are involved not only in the induction of iNOS and the synthesis of acute phase proteins such as AGP, but also in mediating CYP downregulation (2,29,30). Since the observed decrease in P450 expression/activities triggered by FCA administration was accompanied by an increase in NO and AGP production, we proceeded to characterize the time-course of IL-1β, IL-6, and TNF-α in plasma obtained from control and FCA-treated rats. At any time point, there was no significant difference in IL-1β and TNF-α plasma levels between FCA-treated and control rats. In contrast, IL-6 was significantly increased in plasma from FCA-treated rats compared to controls at 8h post-injection. These findings are in agreement with literature reports where IL-1β and TNF-α levels were found to be drastically increased locally (in the rat hindpaw) but not systemically (in plasma) following FCA treatment (5,31). This was also the case in turpentine-treated rats, where IL-1β and TNF-α serum concentrations did not change compared to control rats (32,33). The authors also measured IL-6 circulating levels and these were found to peak at the same time postinjection (8 h) as in our study after FCA administration. Together these findings suggest that IL-6 plays an important role in selectively altering the expression of hepatic P450s in FCA-treated rats. However, it does not preclude the involvement of IL-1β and TNF-α as pro-inflammatory cytokines are often sequentially formed, TNF-α being typically made first, causing the induction of IL-1β, which in turn causes the induction of IL-6 (34).

Several studies support the role of IL-6 (without excluding the involvement of TNF-α and IL-1β). Experiments in turpentine-treated or control rabbits have demonstrated that serum IL-6 was able to decrease total P450 contents in hepatocytes obtained from the turpentine-treated group (35,36). *In vitro*, the incubation of primary cultures of rat hepatocytes with IL-6 was associated with a decrease in CYP2C11 and CYP2B mRNA and/or protein levels (37,38). In rat hepatoma cells, CYP2E1 mRNA and protein were strongly decreased by IL-6 treatment after 24 and 72h, respectively (24). *In vivo*, IL-6 administration decreased CYP2C11 mRNA/proteincontents, but had no effect on CYP3A2 protein levels (39). Finally, in IL-6 knockout mice, the mRNA contents of many P450s (Cyp1a2, Cyp2a5, and Cyp3a11) were not affected by turpentine treatment, which further corroborates the predominant role of IL-6 in P450 downregulation following an inflammatory stimulus (40).

The mechanism(s) by which IL-6 would trigger a decrease in CYP expression is likely to involve important nuclear receptors or liver-enriched transcription factors. In human hepatocytes, IL-6 downregulated PXR and CAR expression (41). During inflammation, the effect of IL-6 on acute phase proteins is thought to be mainly mediated through signal transducers and activators of transcription and/or members of the CCAAT/enhancer binding protein family (42). For example, IL-6 was shown to downregulate the constitutive expression of C/EBPα and enhance the expression of C/EBPβ and C/EBPβ-LIP (43). IL-6 is also one of the strongest inducers of STAT3 activation and the increased expression of STAT3 detected 4h after LPS administration to rats is thought to be mediated by cytokines such as IL-6 (20,26). Because different CYPs could be differentially regulated by one or more of these effectors, the overlapping interplay between nuclear receptors (e.g., PXR or CAR) and transcription factors (e.g., C/EBPs and/or STAT3) may determine the susceptibility of individual CYPs to pro-inflammatory cytokines or various inflammatory stimuli.

In conclusion, our study demonstrates that a single FCA injection in the rat hindpaw leads to the development of an acute inflammatory response, as evidenced by paw edema and increased AGP, NOx and IL-6 plasma levels in the early days that follow FCA injection. These changes are accompanied by a rapid decrease in total P450 contents in rat liver and the selective downregulation of specific CYP isoforms, as illustrated by decreased expression and/or activities in CYP2B, CYP2C6, CYP2C11, and CYP2E1 in FCA-treated rat liver microsomes. These early biochemical modifications may have important consequences when hepatically-cleared drugs are administered to FCA-treated rats within the first 24–72 h post-FCA, as it is the case in the FCA hyperalgesia model. Given the large heterogeneity of pharmacodynamic models used in pain research, ranging from acute tests with marked responses to a short-lasting inflammatory stimulus to more chronic-like conditions, a better biochemical and metabolic characterization of each model would allow us to explain pharmacokinetic, and eventually pharmacodynamic variability, and improve the pharmacokinetic/pharmacodynamic relationships of new chemical entities.

ACKOWLEDGEMENT

AstraZeneca R&D Montreal is acknowledged for Studentship assistance to Denis Projean.

REFERENCES

1. E. T. Morgan, M. B. Sewer, H. Iber, F. J. Gonzalez, Y. H. Lee, R. H. Tukey, S. Okino, T. Vu, Y. H. Chen, J. S. Sidhu, and C. J. Omiecinski. Physiological and pathophysiological regulation of cytochrome P450. *Drug Metab. Dispos.* **26**:1232–1240 (1998).
2. E. T. Morgan. Regulation of cytochromes P450 during inflammation and infection. *Drug Metab. Rev.* **29**:1129–1188 (1997).
3. T. L. Yaksh. Spinal systems and pain processing: development of novel analgesic drugs with mechanistically defined models. *Trends Pharmacol. Sci.* **20**:329–337 (1999).
4. G. L. Fraser, G. A. Gaudreau, P. B. Clarke, D. P. Menard, and M. N. Perkins. Antihyperalgesic effects of delta opioid agonists in a rat model of chronic inflammation. *Br. J. Pharmacol.* **129**:1668–1672 (2000).
5. C. J. Woolf, A. Allchorne, B. Safieh-Garabedian, and S. Poole. Cytokines, nerve growth factor and inflammatory hyperalgesia: the contribution of tumour necrosis factor alpha. *Br. J. Pharmacol.* **121**:417–424 (1997).
6. R. P. Carlson and P. B. Jacobson. Comparison of adjuvant and streptococcal cell wall-induced arthritis. In D. W. Morgan and L. A. Marshall (eds.), *In Vivo Models of Inflammation*. Birkhäuser, Boston, 1999, pp. 1–50.
7. A. Toda, N. Ishii, T. Kihara, A. Nagamatsu, and H. Shimeno. Effect of adjuvant-induced arthritis on hepatic drug metabolism in rats. *Xenobiotica* **24**:603–611 (1994).
8. R. E. Pearce, C. J. McIntyre, A. Madan, U. Sanzgiri, A. J. Draper,

P. L. Bullock, D. C. Cook, L. A. Burton, J. Latham, C. Nevins, and A. Parkinson. Effects of freezing, thawing, and storing human liver microsomes on cytochrome P450 activity. *Arch. Biochem. Biophys.* **331**:145–169 (1996).
9. T. Omura and R. Sato. The carbon monoxide-binding pigment of liver microsomes. I. Evidence for its hemoprotein nature. *J. Biol. Chem.* **239**:2370–2378 (1964).
10. P. M. Whalley, D. Bakes, K. Grime, and R. J. Weaver. Rapid high-performance liquid chromatographic method for the separation of hydroxylated testosterone metabolites. *J. Chromatogr. B.* **760**:281–288 (2001).
11. M. B. Sewer and E. T. Morgan. Down-regulation of the expression of three major rat liver cytochrome P450S by endotoxin in vivo occurs independently of nitric oxide production. *J. Pharmacol. Exp. Ther.* **287**:352–358 (1998).
12. A. J. Sonderfan, M. P. Arlotto, D. R. Dutton, S. K. McMillen, and A. Parkinson. Regulation of testosterone hydroxylation by rat liver microsomal cytochrome P-450. *Arch. Biochem. Biophys.* **255**:27–41 (1987).
13. E. T. Morgan. Suppression of constitutive cytochrome P-450 gene expression in livers of rats undergoing an acute phase response to endotoxin. *Mol. Pharmacol.* **36**:699–707 (1989).
14. Z. Szekanecz, M. M. Halloran, M. V. Volin, J. M. Woods, R. M. Strieter, H. G. Kenneth III, S. L. Kunkel, M. D. Burdick, and A. E. Koch. Temporal expression of inflammatory cytokines and chemokines in rat adjuvant-induced arthritis. *Arthritis Rheum.* **43**:1266–1277 (2000).
15. M. B. Sewer, D. R. Koop, and E. T. Morgan. Differential inductive and suppressive effects of endotoxin and particulate irritants on hepatic and renal cytochrome P-450 expression. *J. Pharmacol. Exp. Ther.* **280**:1445–1454 (1997).
16. M. B. Sewer, D. R. Koop, and E. T. Morgan. Endotoxemia in rats is associated with induction of the P4504A subfamily and suppression of several other forms of cytochrome P450. *Drug Metab. Dispos.* **24**:401–407 (1996).
17. O. Khatsenko and Y. Kikkawa. Nitric oxide differentially affects constitutive cytochrome P450 isoforms in rat liver. *J. Pharmacol. Exp. Ther.* **280**:1463–1470 (1997).
18. T. Li-Masters and E. T. Morgan. Down-regulation of phenobarbital-induced cytochrome P4502B mRNAs and proteins by endotoxin in mice: independence from nitric oxide production by inducible nitric oxide synthase. *Biochem. Pharmacol.* **64**:1703–1711 (2002).
19. V. Nedelcheva and I. Gut. P450 in the rat and man: methods of investigation, substrate specificities and relevance to cancer. *Xenobiotica* **24**:1151–1175 (1994).
20. A. L. Roe, G. Warren, G. Hou, G. Howard, S. I. Shedlofsky, and R. A. Blouin. The effect of high dose endotoxin on CYP3A2 expression in the rat. *Pharm. Res.* **15**:1603–1608 (1998).
21. J. M. Huss, S. I. Wang, and C. B. Kasper. Differential glucocorticoid responses of CYP3A23 and CYP3A2 are mediated by selective binding of orphan nuclear receptors. *Arch. Biochem. Biophys.* **372**:321–332 (1999).
22. A. Mahnke, D. Strotkamp, P. H. Roos, W. G. Hanstein, G. G. Chabot, and P. Nef. Expression and inducibility of cytochrome P450 3A9 (CYP3A9) and other members of the CYP3A subfamily in rat liver. *Arch. Biochem. Biophys.* **337**:62–68 (1997).
23. T. E. Akiyama and F. J. Gonzalez. Regulation of P450 genes by liver-enriched transcription factors and nuclear receptors. *Biochim. Biophys. Acta* **1619**:223–234 (2003).
24. J. Hakkola, Y. Hu, and M. Ingelman-Sundberg. Mechanisms of down-regulation of CYP2E1 expression by inflammatory cytokines in rat hepatoma cells. *J. Pharmacol. Exp. Ther.* **304**:1048–1054 (2003).
25. K. W. Renton. Alteration of drug biotransformation and elimination during infection and inflammation. *Pharmacol. Ther.* **92**: 147–163 (2001).
26. C. Fang, S. Yoon, N. Tindberg, H. A. Jarvelainen, K. O. Lindros, and M. Ingelman-Sundberg. Hepatic expression of multiple acute phase proteins and down-regulation of nuclear receptors after acute endotoxin exposure. *Biochem. Pharmacol.* **67**:1389–1397 (2004).
27. D. E. Amacher and S. J. Schomaker. Ethylmorphine N-demethylase activity as a marker for cytochrome P450 CYP3A activity in rat hepatic microsomes. *Toxicol. Lett.* **94**:115–125 (1998).
28. B. Oesch-Bartlomowicz and F. Oesch. Cytochrome-P450 phosphorylation as a functional switch. *Arch. Biochem. Biophys.* **409**: 228–234 (2003).
29. J. MacMicking, Q. W. Xie, and C. Nathan. Nitric oxide and macrophage function. *Annu. Rev. Immunol.* **15**:323–350 (1997).
30. H. Moshage. Cytokines and the hepatic acute phase response. *J. Pathol.* **181**:257–266 (1997).
31. T. A. Samad, K. A. Moore, A. Sapirstein, S. Billet, A. Allchorne, S. Poole, J. V. Bonventre, and C. J. Woolf. Interleukin-1beta-mediated induction of Cox-2 in the CNS contributes to inflammatory pain hypersensitivity. *Nature* **410**:471–475 (2001).
32. A. L. Cooper, S. Brouwer, A. V. Turnbull, G. N. Luheshi, S. J. Hopkins, S. L. Kunkel, and N. J. Rothwell. Tumor necrosis factor-alpha and fever after peripheral inflammation in the rat. *Am. J. Physiol.* **267**:R1431–R1436 (1994).
33. G. N. Luheshi, A. Stefferl, A. V. Turnbull, M. J. Dascombe, S. Brouwer, S. J. Hopkins, and N. J. Rothwell. Febrile response to tissue inflammation involves both peripheral and brain IL-1 and TNF-alpha in the rat. *Am. J. Physiol.* **272**:R862–R868 (1997).
34. C. A. Dinarello. In L. R. Watkins and S. F. Maier (eds.), *Cytokins and Pain,* Birkhauser, Basel 1999, pp. 1-19.
35. A. M. Bleau, M. C. Levitchi, H. Maurice, and P. Du Souich. Cytochrome P450 inactivation by serum from humans with a viral infection and serum from rabbits with a turpentine-induced inflammation: the role of cytokines. *Br. J. Pharmacol.* **130**:1777–1784 (2000).
36. A. M. Bleau, P. Maurel, V. Pichette, F. Leblond, and P. du Souich. Interleukin-1beta, interleukin-6, tumour necrosis factor-alpha and interferon-gamma released by a viral infection and an aseptic inflammation reduce CYP1A1, 1A2 and 3A6 expression in rabbit hepatocytes. *Eur. J. Pharmacol.* **473**:197–206 (2003).
37. J. Q. Chen, A. Strom, J. A. Gustafsson, and E. T. Morgan. Suppression of the constitutive expression of cytochrome P-450 2C11 by cytokines and interferons in primary cultures of rat hepatocytes: comparison with induction of acute-phase genes and demonstration that CYP2C11 promoter sequences are involved in the suppressive response to interleukins 1 and 6. *Mol. Pharmacol.* **47**:940–947 (1995).
38. T. J. Carlson and R. E. Billings. Role of nitric oxide in the cytokine-mediated regulation of cytochrome P-450. *Mol. Pharmacol.* **49**:796–801 (1996).
39. E. T. Morgan, K. B. Thomas, R. Swanson, T. Vales, J. Hwang, and K. Wright. Selective suppression of cytochrome P-450 gene expression by interleukins 1 and 6 in rat liver. *Biochim. Biophys. Acta* **1219**:475–483 (1994).
40. E. Siewert, R. Bort, R. Kluge, P. C. Heinrich, J. Castell, and R. Jover. Hepatic cytochrome P450 down-regulation during aseptic inflammation in the mouse is interleukin 6 dependent. *Hepatology* **32**:49–55 (2000).
41. J. M. Pascussi, S. Gerbal-Chaloin, L. Pichard-Garcia, M. Daujat, J. M. Fabre, P. Maurel, and M. J. Vilarem. Interleukin-6 negatively regulates the expression of pregnane X receptor and constitutively activated receptor in primary human hepatocytes. *Biochem. Biophys. Res. Commun.* **274**:707–713 (2000).
42. S. Akira. IL-6-regulated transcription factors. *Int. J. Biochem. Cell Biol.* **29**:1401–1418 (1997).
43. R. Jover, R. Bort, M. J. Gomez-Lechon, and J. V. Castell. Down-regulation of human CYP3A4 by the inflammatory signal interleukin-6: molecular mechanism and transcription factors involved. *FASEB J.* **16**:1799–1801 (2002).